Supplemental material

de Jong et al., https://doi.org/10.1084/jem.20170308

Figure S1. **Clinical presentation of P2, P15, P19, P20, and P23. (A)** P2 (age 46) presented with disseminated flat, reddish, and white pityriasis versicolor-like lesions on the trunk, hyperkeratotic warts on the hand, and seborrheic keratosis-like lesions the forehead. **(B)** P15 (age 58) presented with disseminated flat, reddish, white pityriasis versicolor-like lesions on the hands, knees, and neck. **(C)** P19 (age 12) presented with disseminated flat, pityriasis versicolor-like lesions all over the head, arms, and trunk. See Table S1 for more information. **(D)** P23 (age 22) and P20 (age 47), her father, presented reddish, hyperkeratotic lesions on the face, arms, and trunk that had developed in early childhood. The father subsequently developed basosquamous carcinomas on the forehead. See Table S1 for more information.

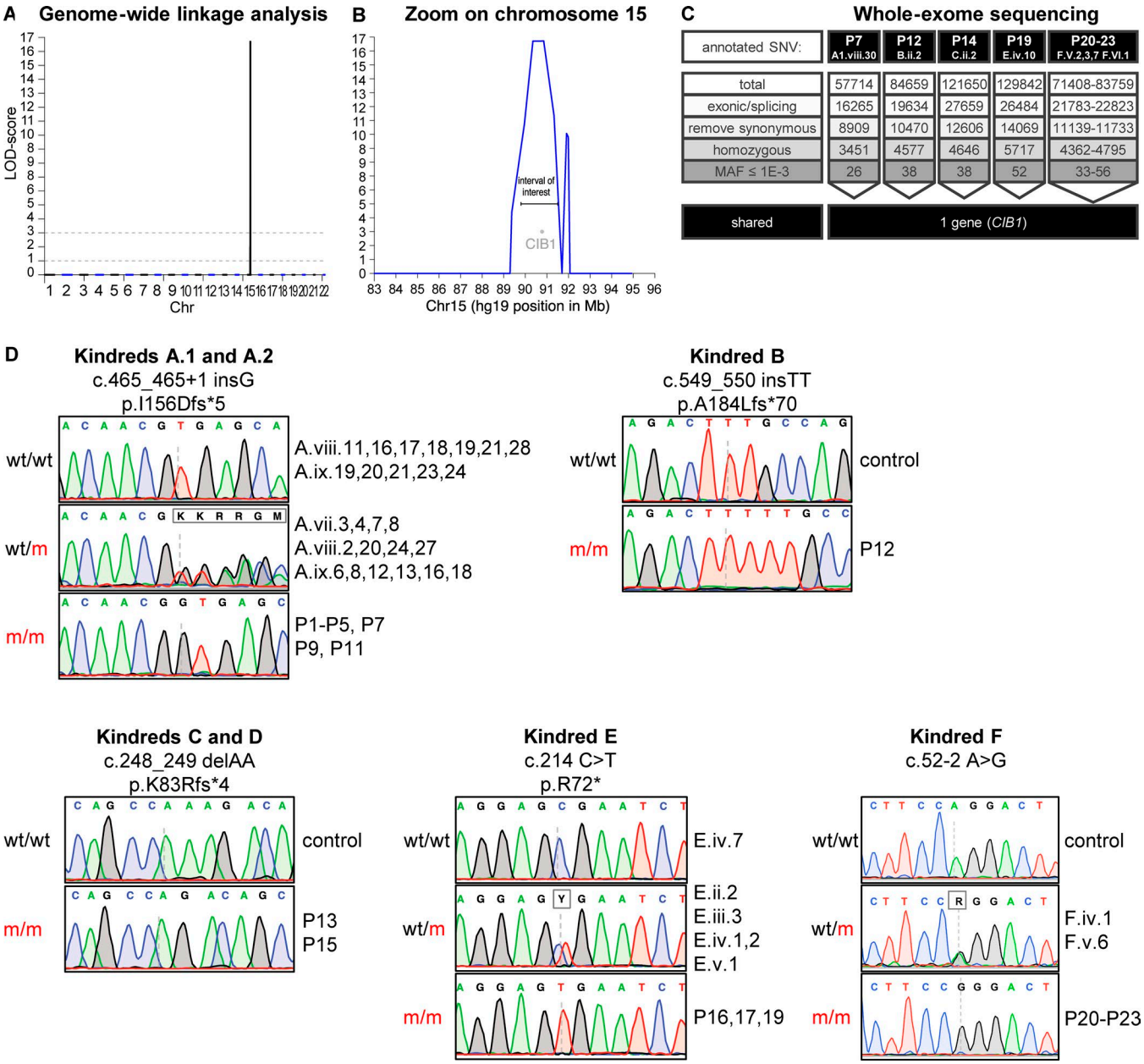

Figure S2. **Combined genome-wide analysis of the EV patients in the cohort analyzed and Sanger sequencing of *CIB1* mutations in six kindreds. (A and B)** Representation of the combined GWL analysis (A) for kindreds A1, B, C, D, E, and F. LOD scores are shown in black and blue for alternate chromosomes. The linkage region with the highest LOD score was on chromosome 15 and contained *CIB1* (B). **(C)** Filtering steps for WES data identified *CIB1* as the only gene carrying homozygous coding mutations in each of P7, P12, P14, P19, and P20–P23. SNV, single-nucleotide variant. **(D)** Sanger sequencing of the *CIB1* mutations (cDNA positions are indicated above the sequence) responsible for the I156D fs*5, A184L fs*70, K83R fs*4, and R73* forms of the CIB1 protein and of the c.52-2 A>G essential splice variant in patients, healthy relatives, and unrelated controls in kindreds A, B, C, D, E, and F (refer to Fig. 1 for individual identifiers).

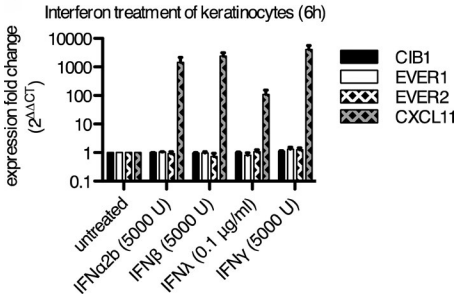

Figure S3. **Induction of *CIB1, EVER1,* and *EVER2* mRNA levels upon IFN stimulations.** Primary keratinocytes from a healthy donor were stimulated with the indicated recombinant proteins at the indicated concentrations for 6 h. Total RNA was isolated and reverse transcribed. *CIB1, EVER1, EVER2,* and *CXCL11* mRNA levels were determined by RT-qPCR. Each bar represents three independent measurements per stimulation. The data were normalized against GAPDH and an unstimulated sample by the ΔΔCt method. *CXCL11* served as a positive control for the biological activity of the recombinant proteins and the ability of the keratinocytes to respond. Error bars represent SD.

A

gene symbol	total peptides	unique peptides	MW (kD)	unique peptides per kD
TMC6	***775***	***34***	***90***	***0.378***
NXF1	100	29	70	0.413
MYH13	82	14	223	0.063
FN1	73	50	262	0.191
CIB1	***57***	***13***	***22***	***0.599***
SMC5	53	45	129	0.350
HUWE1	52	44	482	0.091
SMC6	43	38	126	0.301
HSPG2	42	34	469	0.073
GPRASP2	41	27	94	0.288

B

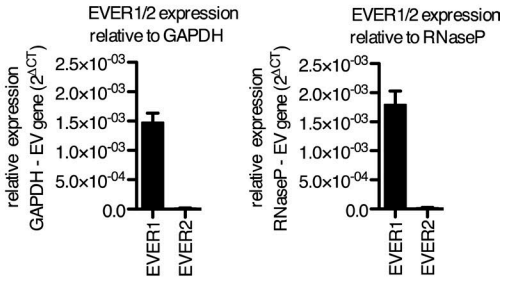

C

Overrepresentation test	Reference		Input		
Reactome pathways (pathway number)	total (21042)	expected proteins	total (244)	fold enrichment	P-value
rRNA modification in the nucleus and cytosol (R-HSA-6790901)	59	0.7	9	13.2	7.7E-05
→ Gene Expression (R-HSA-74160)	1685	19.5	40	2.1	2.2E-02
Viral Messenger RNA Synthesis (R-HSA-168325)	40	0.5	6	12.9	1.6E-02
COPII (Coat Protein 2) Mediated Vesicle Transport (R-HSA-204005)	67	0.8	8	10.3	2.7E-03
→ ER to Golgi Anterograde Transport (R-HSA-199977)	146	1.7	1	6.5	2.6E-03
→ Membrane Trafficking (R-HSA-199991)	529	6.1	23	3.8	1.5E-04
ISG15 antiviral mechanism (R-HSA-1169408)	70	0.8	7	8.6	3.8E-02

D

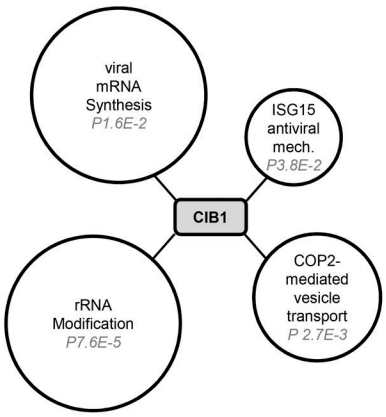

E

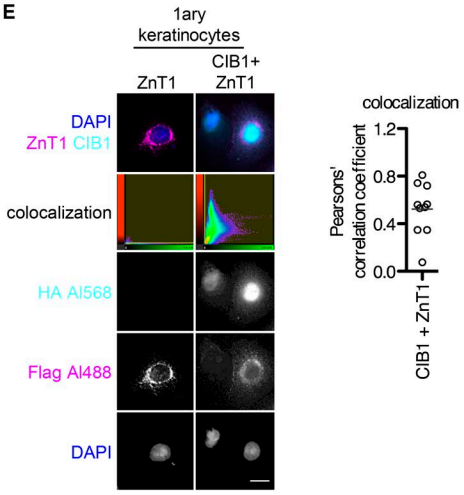

Figure S4. **Mass spectrometry analysis and CIB1-ZnT1 colocalization. (A)** HEK293T cells were transfected with a plasmid encoding CIB1-FLAG. After 36 h, cells were lysed in RIPA buffer and subjected to immunoprecipitation with FLAG-Ezview resin for 4 h. Proteins were separated on 4–12% Bis-Tris gels, which were then stained with colloidal Coomassie blue solution overnight. Unique bands were excised and subjected to mass spectrometry. The hits obtained were pooled and stringently filtered against the CRAPome database. The top 10 hits in terms of total number of peptides detected are presented. MW, molecular weight. **(B)** RNA was isolated from untreated HEK293T cells and reverse transcribed. EVER1 and EVER2 mRNA levels were determined by RT-qPCR. Each bar represents three independent measurement per gene of interest. The data were normalized against two different housekeeping genes: GAPDH and RNaseP. Error bars represent SD. **(C)** Gene ontology PANTHER overrepresentation test. We ran 244 CIB1 interactors identified in A against the Reactome (version 58; released 2016–12-07) database containing 21,042 genes. Bonferroni correction for multiple testing was applied. Fold enrichment and P values <0.05 are displayed. **(D)** Visual representation of B. The size of each cloud corresponds to the fold enrichment for the pathway indicated. P values are indicated within each cloud. **(E)** Primary keratinocytes were transfected with plasmids encoding CIB1-HA and ZnT1-Flag alone or in combination. 1 d after transfection, cells were subjected to immunofluorescence imaging with Alexa Fluor 568–HA and Alexa Fluor 488–FLAG antibody combinations. DAPI was used for counterstaining. Bar, 13 µm. Colocalization was assessed by calculating Pearson's correlation coefficient with Imaris software. All results are representative of three independent experiments.

Table S1. General immunophenotyping on total PBMCs from P3, P5, P15, P16, and P17

A

	P3 A.VIII.10	P5 A.VIII.15	Control range
Lymphocytes total (%)	35.1	46.2	32 (28–39)
T cells $CD3^+$ (%)	69,2	78	67 (50–91)
$CD4^+$ (%)	43.1	37.7	42 (28–64)
Naïve $CCR7^+CD45RA^+/CD4^+$ (%)	27.5	31.5	46 (16–100)
Central memory $CCR7^+CD45RA^-/CD4^+$ (%)	13.5	18.4	42 (18–95)
Effector/ term. diff. $CCR7^-CD45RA^+/CD4^+$ (%)	3.6	4.2	0.35 (0.0083–6.8)
Effector memory $CCR7^-CD45RA^-/CD4^+$ (%)	55.5	45.9	5 (1–23)
$CD8^+$ (%)	21.4	30.7	22 (12–40)
Naïve $CCR7^+CD45RA^+/CD8^+$ (%)	14.8	8.9	29 (6–100)
Central memory $CCR7^+CD45RA^-/CD8^+$ (%)	1.7	1.6	5 (1–20)
Effector/ term. diff. $CCR7^-CD45RA^+/CD8^+$ (%)	32.8	31.5	19 (7–53)
Effector memory $CCR7^-CD45RA^-/CD8^+$ (%)	50.7	58.1	36 (14–98)
$CD4^+/CD8^+$ (%)	0.9	0.8	0.26 (0.075–0.94)
CD4:CD8 ratio	2	1.2	1.9 (1.0–3.6)
B cells			
$CD19^+$ (%)	13.3	12.4	10 (4–28)
$CD19^+/CD21^+$ (%)	12.4	11.9	-
NK cells $CD3^-CD16^+CD56^+$ (%)	11.7	7.7	15 (5–49)
Monocytes $CD45^+CD14^+$ (%)	7.1	5.9	3–8

B

Cell type (%)	P15 D.IV.2	Control range (n = 5)
T cells CD3$^+$	67	75–82
CD4$^+$	40	34–72
Naïve CD45RA$^+$/CD4$^+$	31	27–58
Memory CD45RO$^+$/CD4$^+$	69	43–69
CD8$^+$	47	21–58
Naïve CCR7$^+$CD45RA$^+$/CD8$^+$	7	5–42
Central memory CCR7$^+$CD45RA$^-$/CD8$^+$	6	2–11
Effector/ term. diff. CCR7$^-$CD45RA$^+$/CD8$^+$	61	14–70
Effector memory CCR7$^-$CD45RA$^-$/CD8$^+$	26	18–37
B cells		
CD20$^+$	23	4–15
NK cells CD3$^-$CD16$^+$CD56$^+$	5	4–8

C

Total number per ml	P3 A.VIII.10	P5 A.VIII.15	P16 E.IV.4	P17 E.IV.6	Control range
T cells CD3$^+$	2,240	1,389	1,155	882	1,500 (780–3,000)
CD4$^+$	1,082	865	705	448	1,000 (500–2,000)
CD8$^+$	881	430	315	266	500 (200–1,200)
B cells CD19+	356	267	225	308	230 (64–820)
NK cells CD3$^-$CD16$^+$CD56$^+$	220	235	15	168	340 (100–1,200)

(A) Values for the indicated leukocyte subsets for P3 and P5 are shown in comparison to standard control ranges. **(B)** Values for the indicated leukocyte subsets for P15 are shown in comparison to the range for five healthy donors processed in parallel. **(C)** Lymphocytes counts in P3, P5, P16, and P17 relative to standard control ranges.

Table S2. T-cell proliferation after anti-CD3 antibody stimulation for P3 and P5

T cell proliferation	P3 A.VIII.10	P5 A.VIII.15	Controls ($n = 2$)
Proliferation index (average number of divisions in dividing cell population)			
Nonstimulated	2.08	2.03	2.67 (1.73–1.88)
1.25 µg/ml α-CD3	1.96	1.96	2.23 (2.22–2.25)
2.5 µg/ml α-CD3	1.95	1.95	2.05 (2.04–2.06)
5 µg/ml α-CD3	2.01	2	2.25 (1.95–2.55)
Percent division (percentage of dividing cells)			
Nonstimulated	2.16	4.78	3.86 (3.0–4.7)
1.25 µg/ml α-CD3	36.7	42.6	43.8 (32.2–55.4)
2.5 µg/ml α-CD3	42.8	40.6	44.3 (40.6–48)
5 µg/ml α-CD3	43.5	48.6	41.45 (34.4–48.5)
Division index (average number of divisions in total cell population)			
Nonstimulated	0.045	0.097	0.068 (0.05–0.08)
1.25 µg/ml α-CD3	0.72	0.837	0.977 (0.72–1.23)
2.5 µg/ml α-CD3	0.832	0.791	0.908 (0.83–0.98)
5 µg/ml α-CD3	0.875	0.971	0.911 (0.87–0.94)

T cells from P3 and P5 were stimulated with an anti-CD3 antibody, and T-cell proliferation was assessed by comparison with that in two healthy donors.

Table S3. Titers of antibodies against common DNA and RNA viral antigens in kindred A1

Individual	Age	CIB1 I156fs*5	DNA viruses							RNA viruses				
			HSV-1	HSV-2	VZV	CMV	EBV EBNA	HBV Ab HBs	HBV Ag HBs	HAV	HCV	Measles	Rubella	Mumps
			Index	Index	IU/ml	AU/ml	AU/ml	U/ml	U/ml	Index	Index	AU/ml	AU/ml	U/ml
A.viii.11	45	wt/wt	52	N	1.17	>180	96	N	N	11	N	34	42	63
A.viii.16	33	wt/wt	56	N	1.50	148	160	N	N	14	N	85	105	113
A.viii.17	32	wt/wt	42	N	1.02	64	340	N	N	14	N	21	15	N
A.viii.18	?	wt/wt	9	N	1.60	84	350	nt	nt	nt	nt	nt	nt	nt
A.viii.19	29	wt/wt	21	5	0.60	105	>600	N	N	14	N	N	24	60
A.ix.19	4	wt/wt	N	N	N	N	N	nt	nt	nt	nt	nt	nt	nt
A.vii.3	74	wt/m	61	N	0.70	112	430	70	N	15	N	>300	16	28
A.vii.4	68	wt/m	32	11	1.89	90	390	46	N	13	N	>300	17	72
A.ix.8	20	wt/m	40	N	1.50	40	47	N	N	15	N	110	DT	25
A.ix.12	20	wt/m	N	N	2.50	76	550	14	N	14	N	260	15	23
A.ix.13	18	wt/m	N	N	1.60	N	>600	N	N	N	N	225	34	80
A.ix.6	4	wt/m	50	N	N	36	>600	nt	nt	nt	nt	nt	nt	nt
P1 A.viii.4	48	m/m	45	1	0.90	60	200	N	P	10	N	40	90	75
P2 A.viii.7	46	m/m	62	10	2.20	80	N	N	P	14	N	>300	300	>300
P3 A.viii.10	44	m/m	48	N	1.40	140	80	N	P	11	N	250	32?	>300
P4 A.viii.12	42	m/m	40	N	1.70	100	200	N	P	10	N	65	45	55
P5 A.viii.15	34	m/m	31	N	1.20	127	>600	N	N	15	N	20	55	290

Serum samples from patients P1–P5 and healthy family members (WT [wt/wt] or heterozygous [wt/m] for CIB1 I156D fs*5) were tested for the presence of antibodies against herpes simplex virus (HSV)-1 and -2, varicella zoster virus (VZV), human CMV, EBV, hepatitis B virus (HBV), hepatitis A virus (HAV), hepatitis C virus (HCV), measles, rubella, and mumps. Titers were normal for all antigens tested. **N, negative**; **P, positive**; **nt,** not tested.

Table S4. Skin-homing T cell subsets in kindred A1 and P15

Skin-homing T cell populations	Controls	Kindred A			D.IV.2	$RHOH^{-/-}$
	n = 5	*n* = 5	*n* = 4	*n* = 4	P15	
Genotype CIB1 (%)	wt/wt	wt/wt	wt/m	m/m	m/m	
$CD3^+$						
CLA^+	7–17	7–9	8–10	6–12	13	4
CLA^+CCR4^+	3–10	1–3	3–4	3–6	7	1
CLA^+CCR10^+	0–2	2–3	1–3	1–1.5	1.3	0.2
$CCR10^+$	3–11	6–23	7–22	11–19	22	5
$CD4^+$						
CLA^+	12–19	8–13	8–17	8–14	17	4
CLA+$CCR4^+$	6–13	3–8	6–10	4–8	11	2
CLA^+CCR10^+	3–5	1–3	2–4	1–3	2.8	0.5
$CCR10^+$	1–7	3–5	3–9	2–4	4	0.6
$CD8^+$						
CLA^+	4–15	2–14	6–9	4–10	9	3
CLA^+CCR4^+	1–8	1–14	1–3	2–5	4	1
CLA^+CCR10^+	0–4	0–1	2–4	1–3	0.2	0.02
$CCR10^+$	0–2	0–4	0–10	0.2–0.7	0.3	0.1

Total PMBCs from kindred A1 (P1–P4; healthy family members [WT (wt/wt) or heterozygous (wt/m) for CIB1 I156D fs*5]), P15, and a RHOH-deficient patient were stained for the indicated skin-homing T cell subsets. Values are shown relative to the range for five healthy donors that were processed in parallel. Deviations from reference values are highlighted in red.

Table S5. Calculation of the inbreeding coefficient (F)

CIB1 mutation	I156D fs*5							A184Lfs*70	K83Rfs*4		R72*			c.52-2G>A			
Patient	**P1**	**P2**	**P3**	**P4**	**P5**	**P7**	**P11**	**P12**	**P14**	**P15**	**P16**	**P17**	**P19**	**P20**	**P21**	**P22**	**P23**
	A.VIII.4	**A.VIII.7**	**A.VIII.10**	**A.VIII.12**	**A.VIII.15**	**A.VIII.30**	**A.II.13**	**B.II.2**	**C.II.2**	**D.IV.2**	**E.IV.4**	**E.IV.6**	**E.IV.10**	**F.V.2**	**F.V.3**	**F.V.7**	**F.VI.1**
Reported degree of parental consanguinity			**5th**			**?**	**?**	**none**	**none**	**1st**		**1st**			**1st**		**2nd**
Consanguinity coefficient (F)	**0,037**	**0,055**	**0,020**	**0,048**	**0,055**	**0,055**	**0,014**	**0,043**	**0,013**	**0,080**	**0,095**	**0,077**	**0,094**	**0,122**	**0,102**	**0,084**	**0,068**
Inferred degree parental consanguinity			**2nd**			**2nd**	**2nd**	**1st**	**2nd**	**double 1st**		**double 1st**			**(double) 1st**		**1st**

Inbreeding coefficients and the inferred degree of parental consanguinity were estimated with the FEstim method (Leutenegger et al., 2003) with FSuite software (Gazal et al., 2014) as described in Materials and methods.

Table S6. Transcriptomics analysis for genes up- and down-regulated in cells from CIB1-deficient patients

Gene name	log2 (fold change [patients vs. controls])
ZP4	3.50
HOXB2	3.43
SPRR2F	3.32
HOXB3	2.60
CTSK	2.43
IL6	2.29
NLRP3	2.19
MMP9	1.87
TGM3	1.69
EMX2	1.58
ANK1	1.41
PROC	1.40
COL22A1	1.36
GCNT2	1.29
MYPN	1.29
CHRNA9	1.28
ITGB6	1.28
EPHX4	1.20
WNT9A	1.18
ADAM19	1.12
EVA1A	1.09
MATN3	1.08
OTUB2	1.08
ALDH1A3	1.06
FOXL2	1.02
TMEM156	1.02
HSD11B1L	−1.03
FGF1	−1.04
LRRC73	−1.07
CIB1	−1.12
GALR2	−1.17
AKT3	−1.26
CXCR2	−1.31

LY6K	−1.34
NPM2	−1.38
ERP27	−1.40
EN1	−1.59
MCOLN3	−1.75
HOXD8	−1.82
PCLO	−3.47

Total RNA was isolated from primary keratinocytes and subjected to mRNA sequencing NextSeq 500 using generating 75-bp single reads. This table shows the log2(fold change) in expression for the comparison of patients to controls. The gene presented were selected in several steps in the isogenic setting. We first filtered on genes differentially regulated between cells from the patients and the same cells transfected with GST considering a log(fold change) threshold of ±1. We then filtered on genes differentially regulated between cells from the patients and the same cells complemented with CIB1 considering a log(fold-change) threshold of ±2.

References

Leutenegger, A.L., B. Prum, E. Genin, C. Verny, A. Lemainque, F. Clerget-Darpoux, and E.A. Thompson. 2003. Estimation of the inbreeding coefficient through use of genomic data. *Am. J. Hum. Genet.* 73:516-523

Gazal, S., M. Sahbatou, M.-C. Babron, E. Génin, and A.L. Leutenegger. 2014. FSuite: exploiting inbreeding in dense SNP chip and exome data. *Bioinforma.* 30:1940–1941